

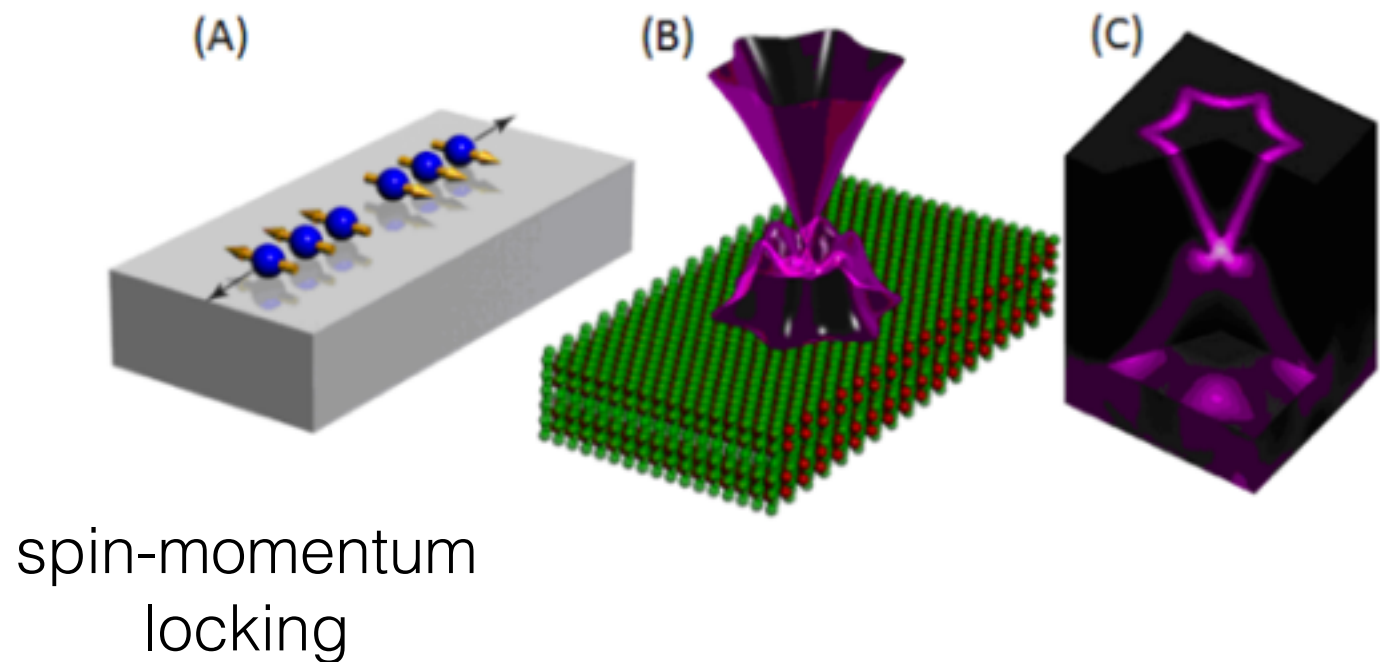
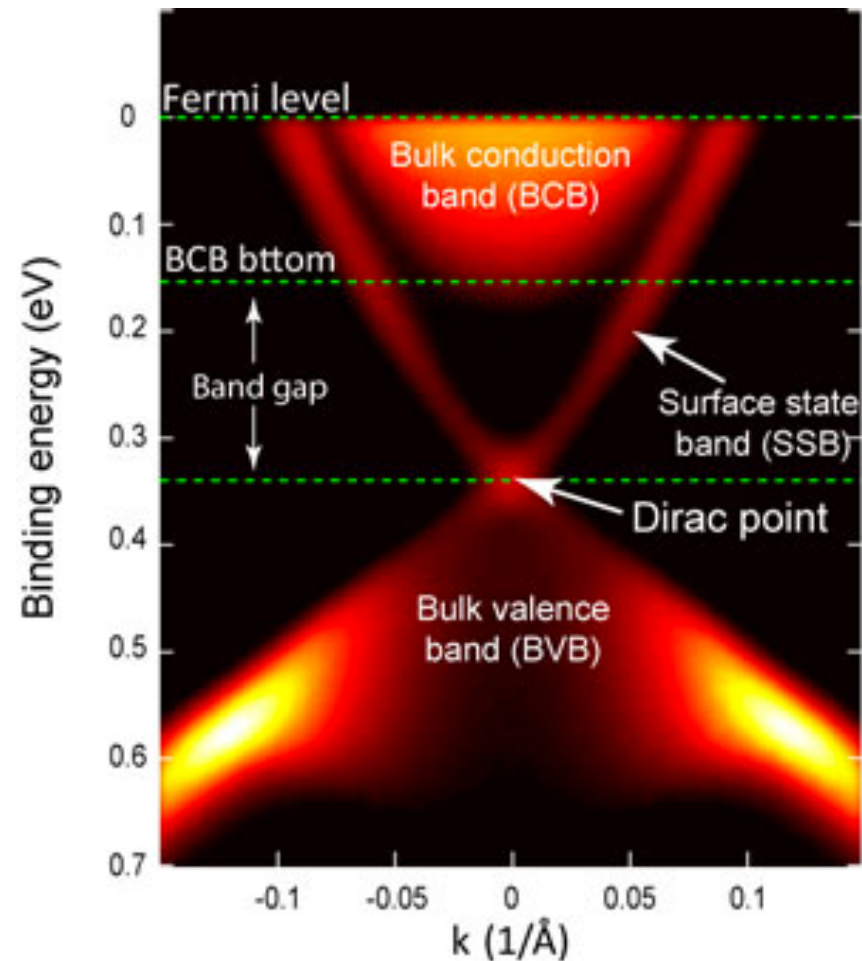
(Some) Frontiers of Quantum Magnetism Theory

Gang Chen
Fudan University

Outline

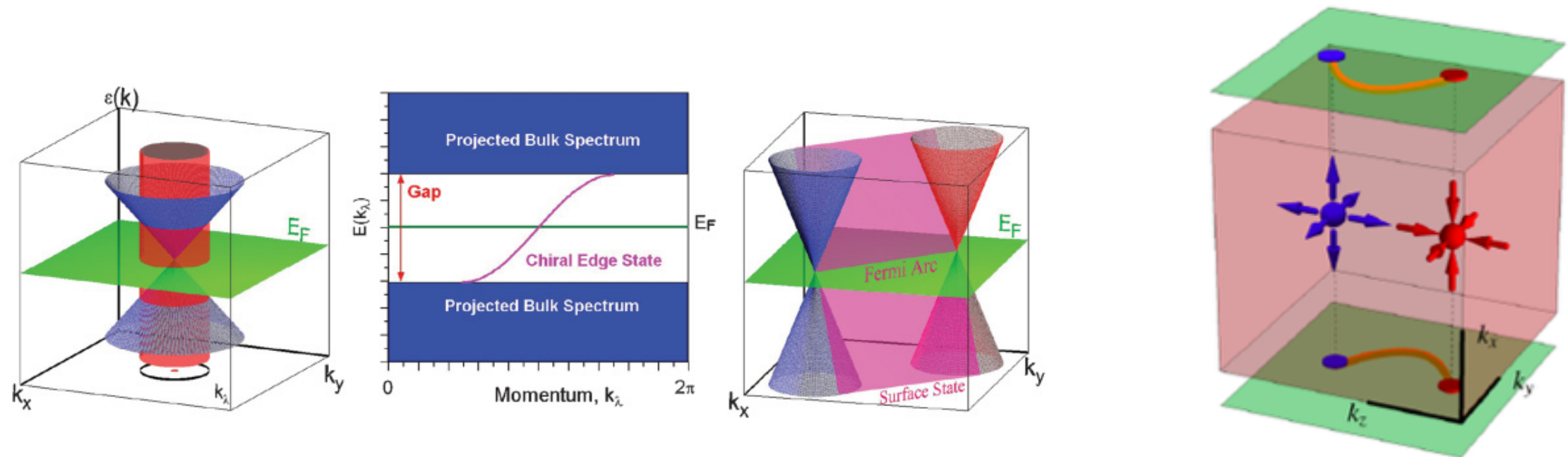
1. Topological (Weyl) magnons: realization and detection
2. Intertwined magnetic multipolar orders and selective measurements

Topological insulator



Surface Dirac cone protected by time reversal symmetry, emerges from bulk-boundary/surface correspondence.

Weyl semimetal



k.p theory

$$H_D = E_0 \mathbb{1} + \mathbf{v}_0 \cdot \mathbf{q} \mathbb{1} + \sum_{i=1}^3 \mathbf{v}_i \cdot \mathbf{q} \sigma_i.$$

Chirality of Weyl node

$$c = \text{sgn}(\mathbf{v}_1 \cdot \mathbf{v}_2 \times \mathbf{v}_3).$$

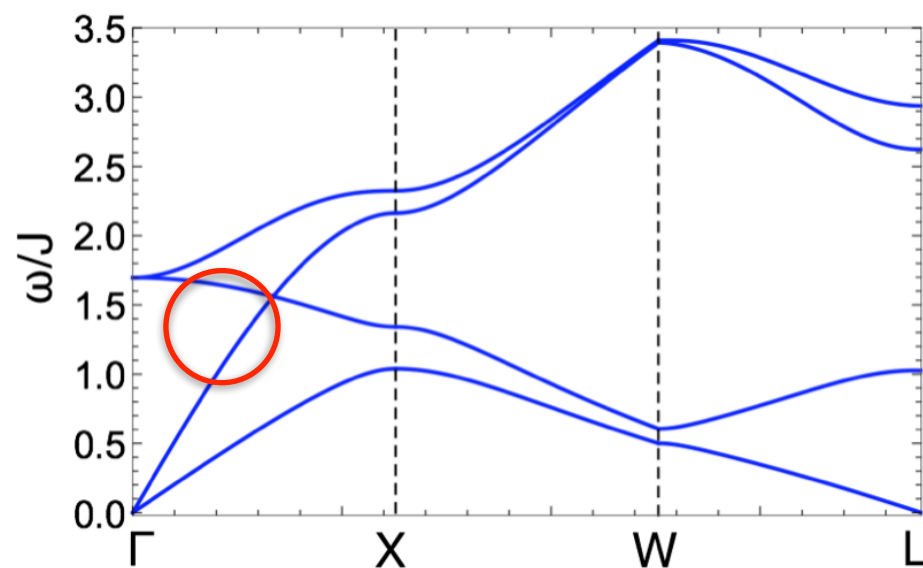
To obtain WSM, one has to break either time reversal or inversion, e.g. TaAs (break inversion), magnetic WSM is not found yet.

Xiangang Wan, AM Turner, Vishwanath, Savrasov, PRB 2011

These are all topological electrons, or electron band topology.
But we are interested in magnetism here.

Where is (this kind of) topology in our field?

Weyl magnons: generalities and specialties



spin-wave spectrum
of a 3D antiferromagnet

Analogous to the Weyl electrons:

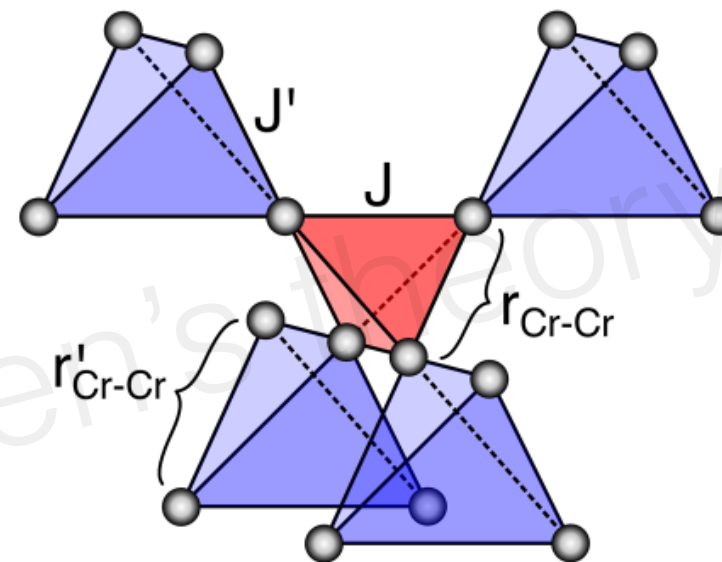
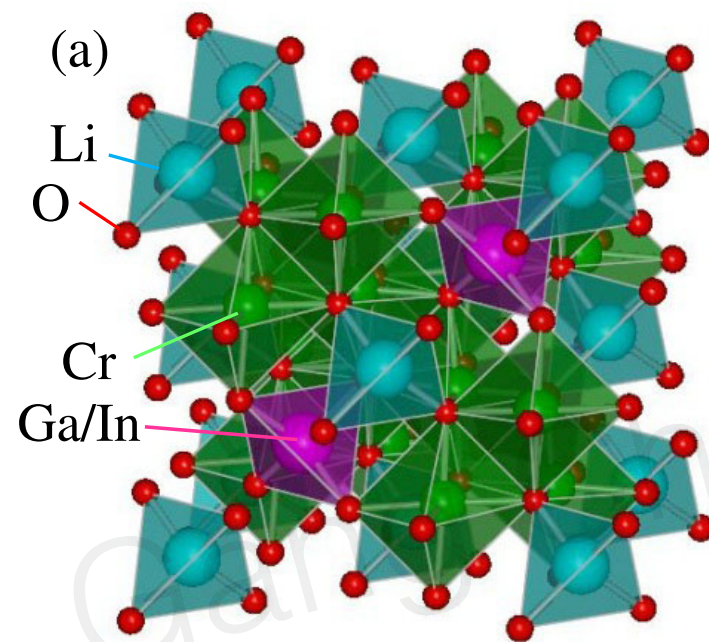
- * bulk-boundary correspondence
- * robust band touching
- * surface arcs

Differs from the Weyl electrons:

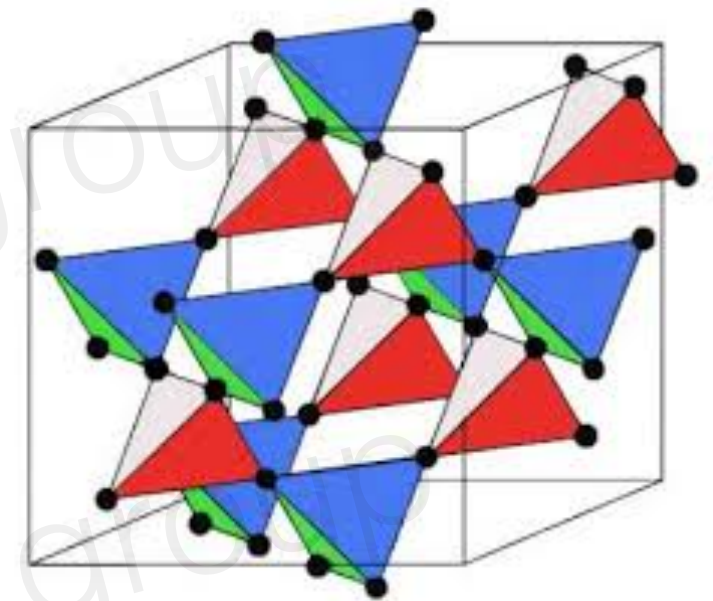
- * charge neutral
- * bosonic, no Fermi surface/energy
- * response to the magnetic field
- * Due to the magnetic order and the spin Hamiltonian

Ref: F-Y Li, Y-D Li, Y Kim, L Balents, Y Yu, G.C.
Nature Comm 2016

Concrete example with breathing pyrochlore



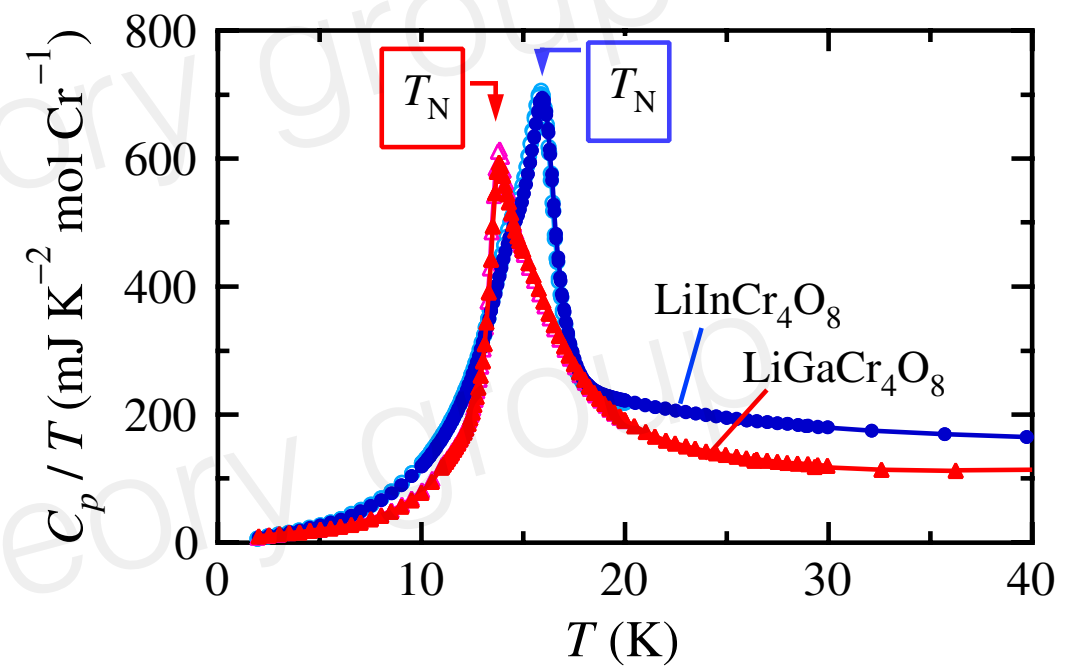
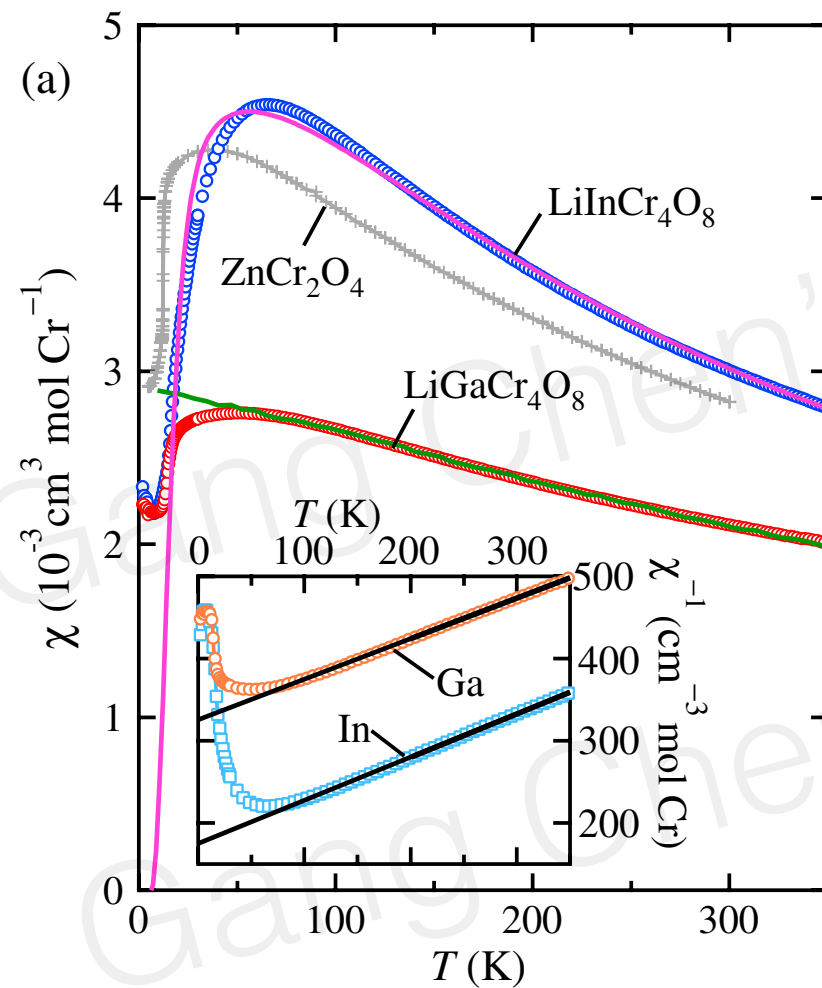
Breathing Pyrochlore



Regular Pyrochlore

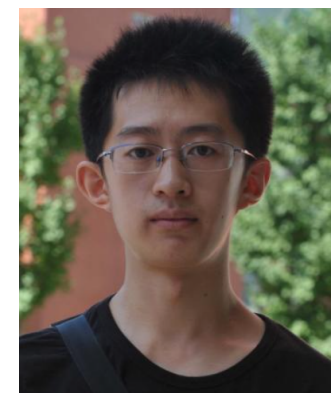
K. Kimura, S. Nakatsuji, and T. Kimura, **PhysRevB** 2014,
Yoshihiko Okamoto, Gørn J. Nilsen, J. Paul Attfield, and Zenji Hiroi, **PhysRevLett** 2013,
Yu Tanaka, Makoto Yoshida, Masashi Takigawa, Yoshihiko Okamoto, and Zenji Hiroi, **PhysRevLett** 2014.

Existing experiments on Cr-based breathing pyrochlores

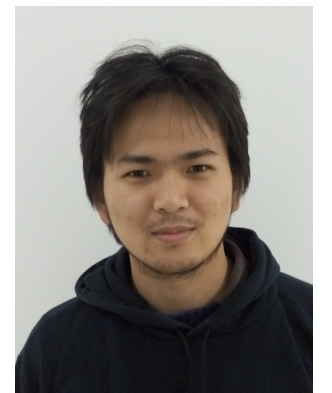


The systems have magnetic orders

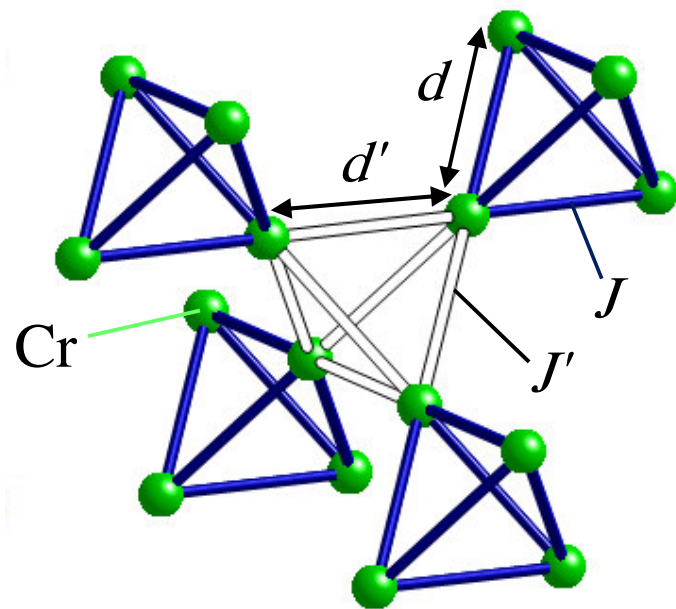
A minimal model



Fei-Ye Li
(Fudan)



Yao-Dong Li
(UCSB)

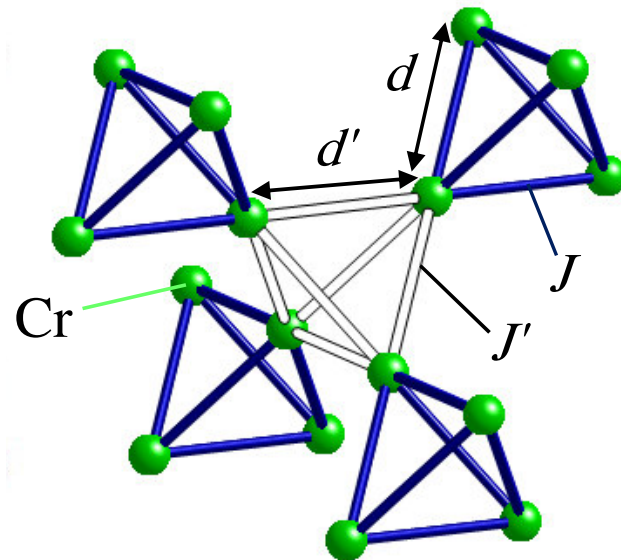


As there is no orbital degeneracy for the $3d^3$ electron configuration of Cr^{3+} ions, the orbital angular momentum is fully quenched and the Cr^{3+} local moment is well described by the total spin $S = 3/2$ via the Hund's rule. As

$$H = J \sum_{\langle ij \rangle \in \text{u}} \mathbf{S}_i \cdot \mathbf{S}_j + J' \sum_{\langle ij \rangle \in \text{d}} \mathbf{S}_i \cdot \mathbf{S}_j + D \sum_i (\mathbf{S}_i \cdot \hat{z}_i)^2,$$

There would also be the Dzyaloshinskii-Moriya interaction due to the absence of inversion symmetry. But let's not worry about it now, since it is subleading.

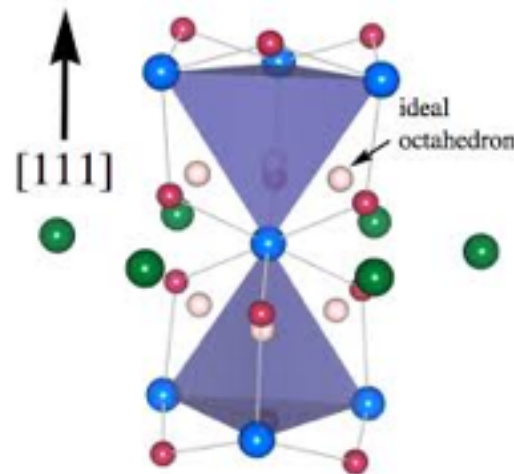
Mean-field ground states



Treating spins as classical vectors, simple algebra gives some rules for ground states

$$\sum_{\langle ij \rangle \in u} \mathbf{S}_i \cdot \mathbf{S}_j \sim \frac{1}{2} \left(\sum_{i \in u} \mathbf{S}_i \right)^2$$

$$\sum_{\langle ij \rangle \in d} \mathbf{S}_i \cdot \mathbf{S}_j \sim \frac{1}{2} \left(\sum_{i \in d} \mathbf{S}_i \right)^2$$



Then worry about the single-ion anisotropy

$$D \sum_i (\mathbf{S}_i \cdot \hat{\mathbf{z}}_i)^2$$

easy-axis vs easy-plane

Easy-plane: order by quantum disorder

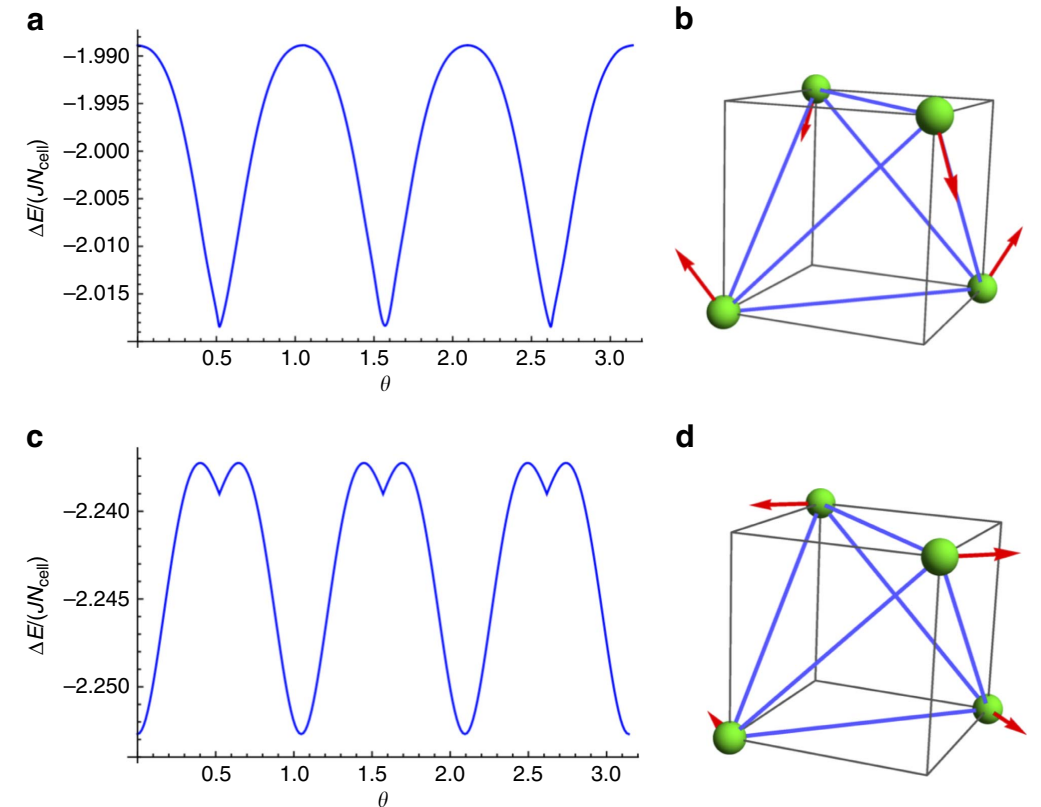
$$\mathbf{S}_i^{\text{cl}} \equiv S\hat{\mathbf{m}}_i = S(\cos \theta \hat{x}_i + \sin \theta \hat{y}_i),$$

$$\mathbf{S}_i \cdot \hat{\mathbf{m}}_i = S - a_i^\dagger a_i,$$

$$\mathbf{S}_i \cdot \hat{\mathbf{z}}_i = (2S)^{1/2} (a_i + a_i^\dagger) / 2,$$

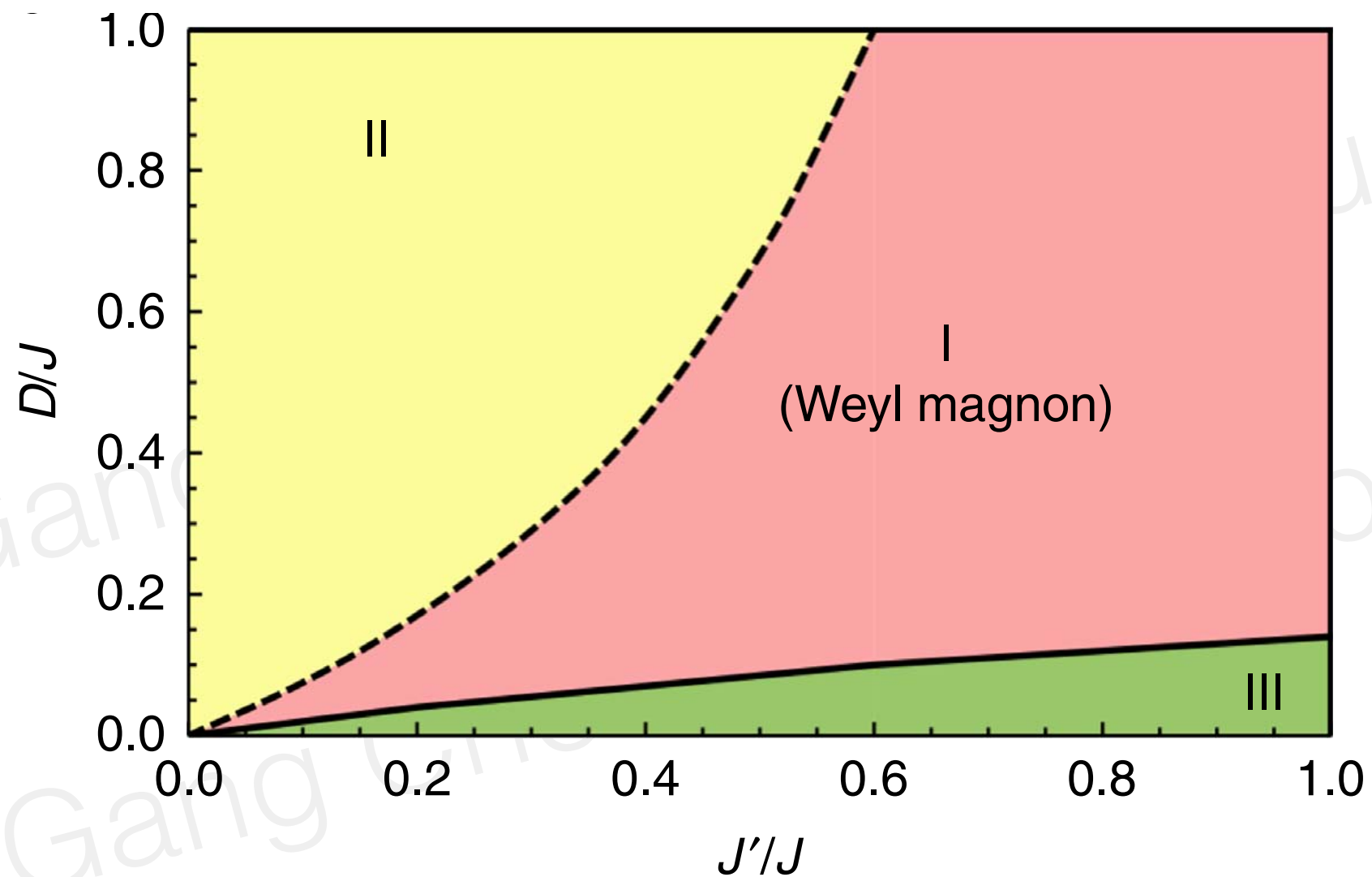
$$\mathbf{S}_i \cdot (\hat{\mathbf{m}}_i \times \hat{\mathbf{z}}_i) = (2S)^{1/2} (a_i - a_i^\dagger) / (2i)$$

$$H_{\text{sw}} = \sum_{\mathbf{k}} \sum_{\mu, \nu} \left[A_{\mu\nu}(\mathbf{k}) a_{k,\mu}^\dagger a_{k,\nu} + B_{\mu\nu}(\mathbf{k}) a_{-k,\mu} a_{k,\nu} \right. \\ \left. + B_{\mu\nu}^*(-\mathbf{k}) a_{k,\mu}^\dagger a_{-k,\nu}^\dagger \right] + E_{\text{cl}},$$



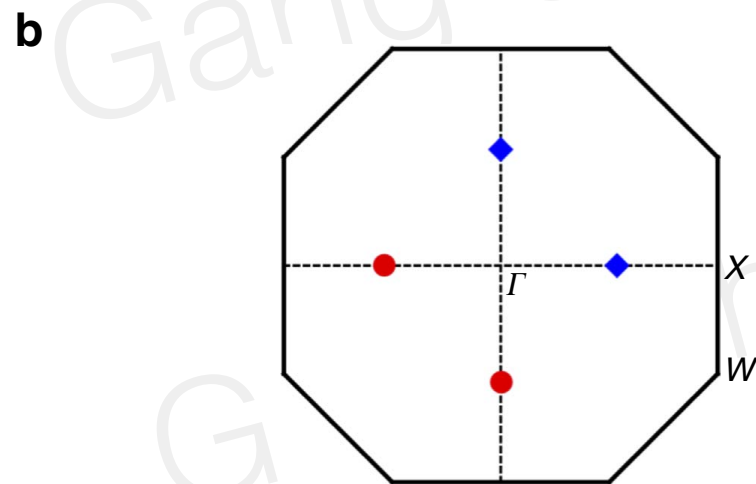
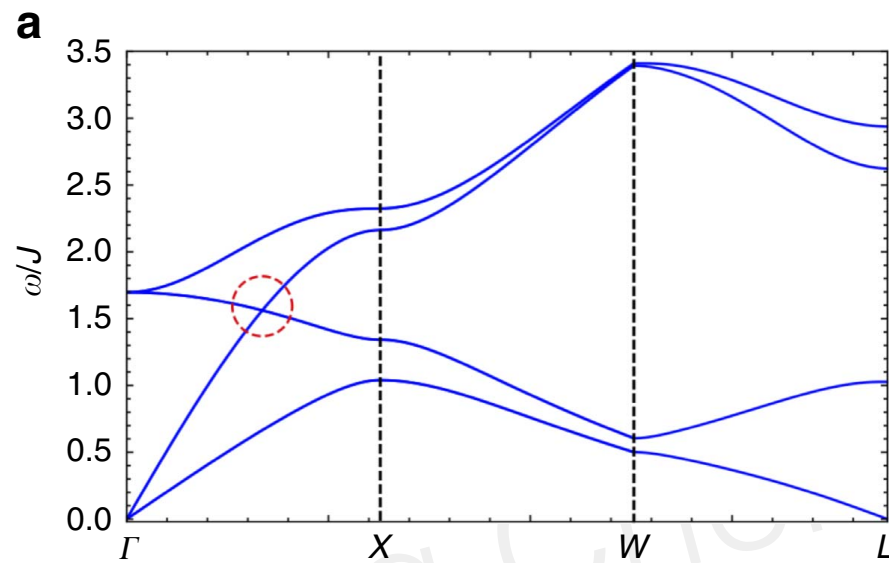
**Selection from quantum
zero-point energy**

Phase diagram

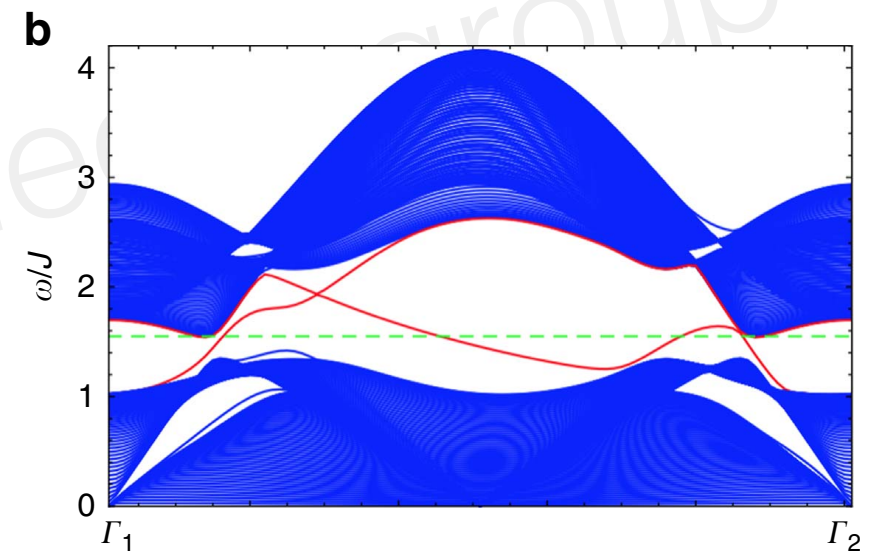
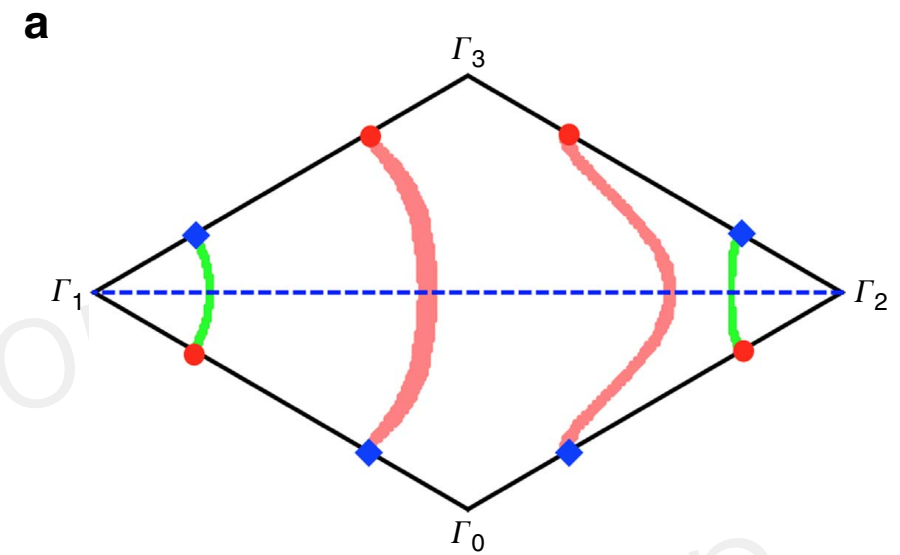


Dashed line is NOT phase boundary.
region I and II are the same phase.

Weyl magnon and surface arcs



Different color means different chirality



| Surface states of a slab. The slab is cleaved along the $[11\bar{1}]$

Response to the magnetic field

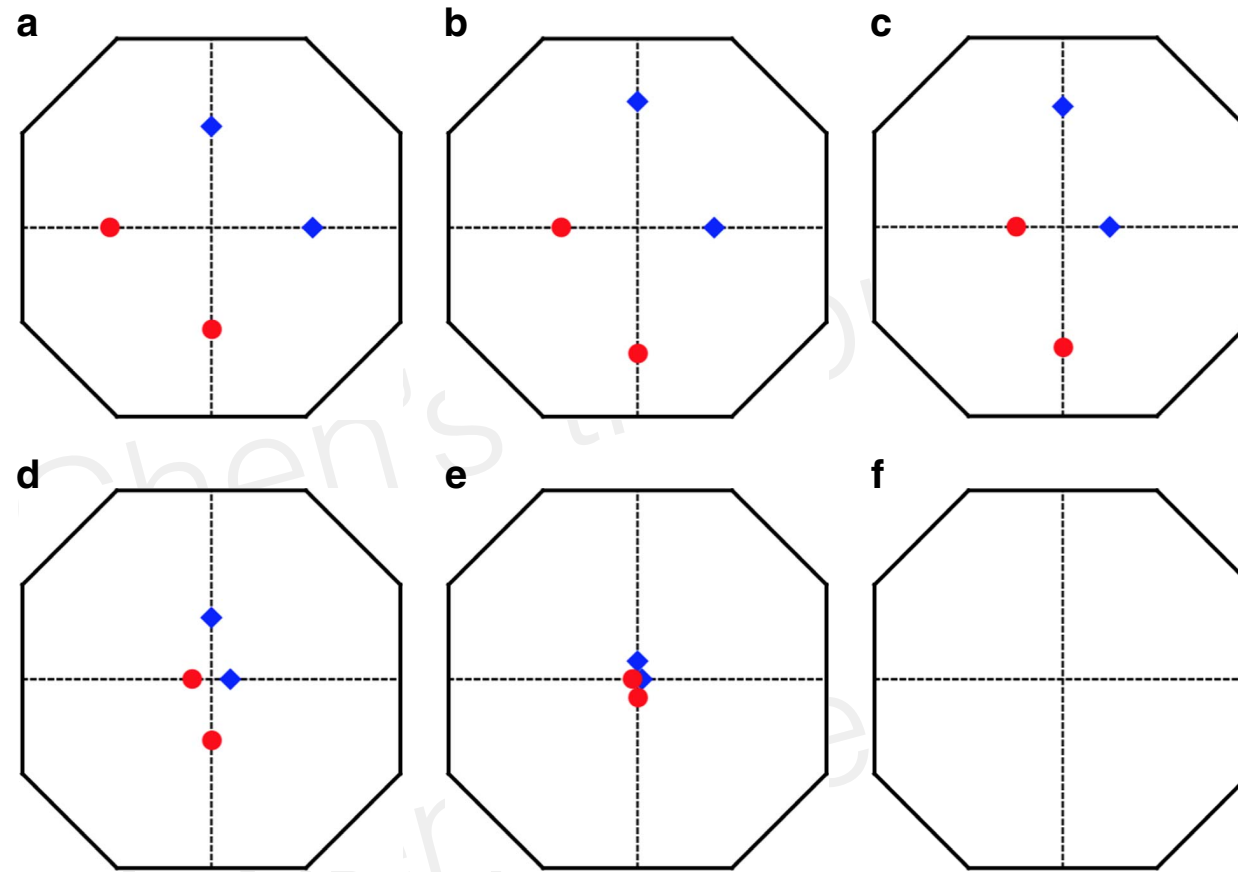


Figure 5 | The evolution of Weyl nodes under the magnetic field. Applying a magnetic field along the global z direction, $\mathbf{B}=B\hat{\mathbf{z}}$, Weyl nodes are shifted but still in $k_z=0$ plane. They are annihilated at Γ when magnetic field is strong enough. Red and blue indicate the opposite chirality. **(a,f)**: $B=0, 0.1J, 0.5J, 0.9J, 1.0J, 1.1J$. We have set $D=0.2J$, $J'=0.6J$ and $\theta=\pi/2$.

How to probe in a REAL experiment?

1. Neutron scattering: detect the Weyl nodes as well as the consequence (the surface arc states that connect the Weyl nodes).
2. Thermal Hall effect: magnon Weyl nodes contribute the thermal currents that are tunable by external magnetic field.
3. Optically: as Weyl node must appear at finite energy, one needs to use pump-probe measurement.

Other pyrochlores

Spin-1 pyrochlore

$\text{Y}_2\text{Ru}_2\text{O}_7$	$\text{Ru}^{4+}(4d^4)$	-1250K	AFM transition at 76K	noncollinear AFM $\mathbf{Q} = \mathbf{0}$
$\text{Tl}_2\text{Ru}_2\text{O}_7$	$\text{Ru}^{4+}(4d^4)$	-956K	structure transition at 120K	gapped paramagnet
$\text{Eu}_2\text{Ru}_2\text{O}_7$	$\text{Ru}^{4+}(4d^4)$	-	Ru order at 118K	Ru order
$\text{Pr}_2\text{Ru}_2\text{O}_7$	$\text{Ru}^{4+}(4d^4), \text{Pr}^{3+}(4f^2)$	-224K	Ru AFM order at 162K	Ru AFM order
$\text{Nd}_2\text{Ru}_2\text{O}_7$	$\text{Ru}^{4+}(4d^4), \text{Nd}^{3+}(4f^3)$	-168K	Ru AFM order at 143K	Ru AFM order
$\text{Gd}_2\text{Ru}_2\text{O}_7$	$\text{Ru}^{4+}(4d^4), \text{Gd}^{3+}(4f^7)$	-10K	Ru AFM order at 114K	Ru AFM order $\mathbf{Q} = \mathbf{0}$
$\text{Tb}_2\text{Ru}_2\text{O}_7$	$\text{Ru}^{4+}(4d^4), \text{Tb}^{3+}(4f^8)$	-16K	Ru AFM order at 110K	Ru AFM order $\mathbf{Q} = \mathbf{0}$
$\text{Dy}_2\text{Ru}_2\text{O}_7$	$\text{Ru}^{4+}(4d^4), \text{Dy}^{3+}(4f^9)$	-10K	Ru AFM order at 100K	Ru AFM order
$\text{Ho}_2\text{Ru}_2\text{O}_7$	$\text{Ru}^{4+}(4d^4), \text{Ho}^{3+}(4f^{10})$	-4K	Ru AFM order at 95K	Ru FM order $\mathbf{Q} = \mathbf{0}$
$\text{Er}_2\text{Ru}_2\text{O}_7$	$\text{Ru}^{4+}(4d^4), \text{Er}^{3+}(4f^{11})$	-16K	Ru AFM order at 92K	Ru AFM order $\mathbf{Q} = \mathbf{0}$
$\text{Yb}_2\text{Ru}_2\text{O}_7$	$\text{Ru}^{4+}(4d^4), \text{Yb}^{3+}(4f^{13})$	-	Ru AFM order at 83K	Ru AFM order
$\text{Y}_2\text{Mo}_2\text{O}_7$	$\text{Mo}^{4+}(4d^2)$	-200K	Mo spin glass at 22K	Mo spin glass
$\text{Lu}_2\text{Mo}_2\text{O}_7$	$\text{Mo}^{4+}(4d^2)$	-160K	Mo spin glass at 16K	Mo spin glass
$\text{Tb}_2\text{Mo}_2\text{O}_7$	$\text{Mo}^{4+}(4d^2), \text{Tb}^{3+}(4f^8)$	20K	spin glass at 25K	spin glass

Spin-3/2 pyrochlore

ular pyrochlore system. Besides the Co-pyrochlore and Cr-spinel, the Mn-pyrochlore ($\text{A}_2\text{Mn}_2\text{O}_7$) is another ideal spin-3/2 system. These materials were studied in the 1990s after the discovery of giant magnetoresistance¹⁸. Since most of these Mn-pyrochlores are well ordered, it would be exciting to explore the topological magnons in these materials.

Ref: F-Y Li, GC, arXiv 1712.00740

Further extension of topological magnons

1. Chern number of 2D magnon bands
2. Dirac magnon
3. Nodal loop magnon

Refs:

Pershoguba, et al. Balatsky, PRX 2018,

KangKang Li, et al. Yuan Li, Chen Fang, PRL 2017,

Max Hirschberger, Robin Chisnell, Young S. Lee, N. P. Ong, PRL 2015

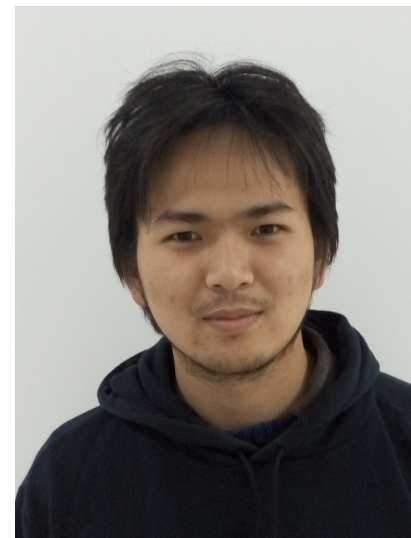
Outline

1. Topological (Weyl) magnons: realization and detection
2. Intertwined magnetic multipolar orders and selective measurements

Selective measurements of intertwined multipolar order on a triangular lattice with non-Kramers doublets



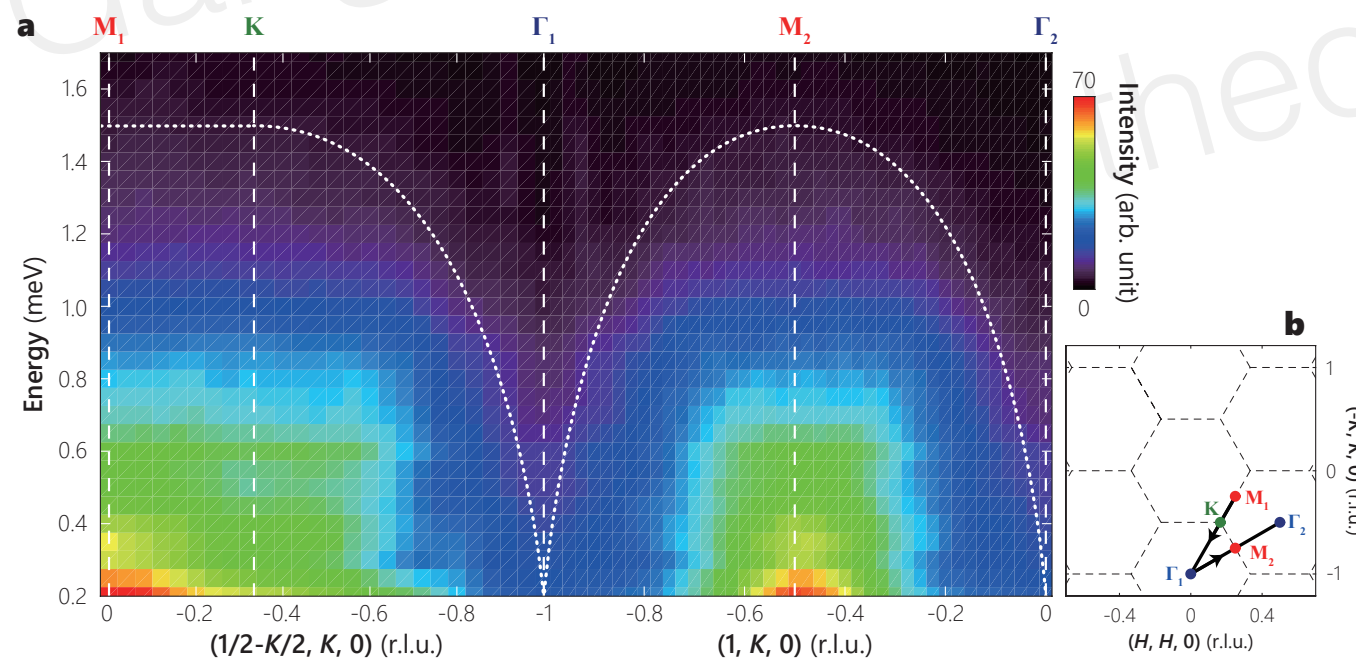
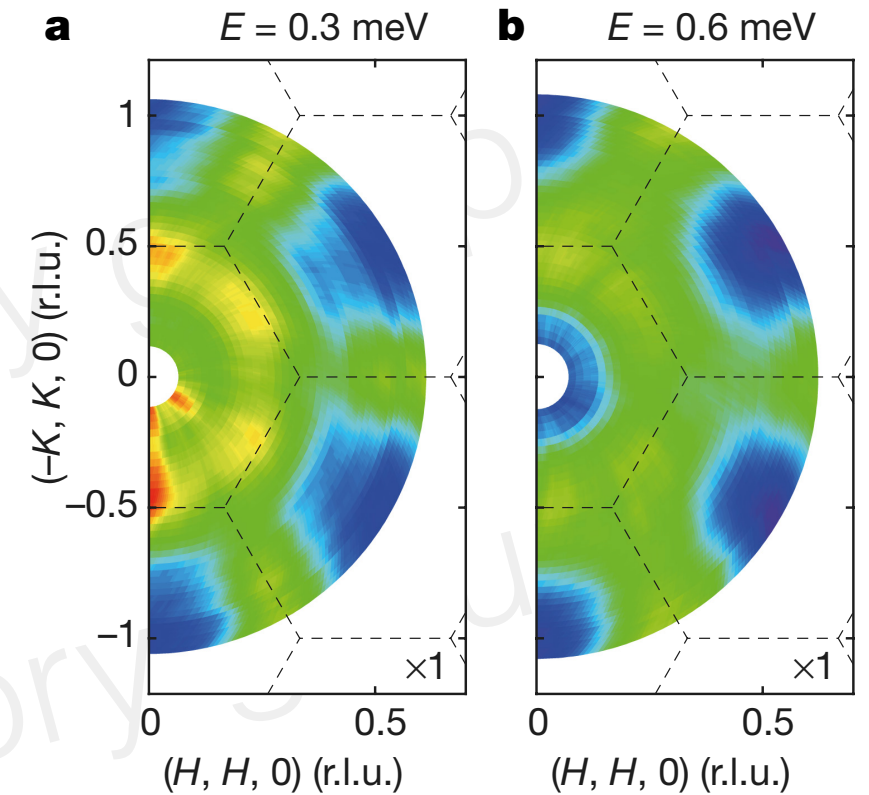
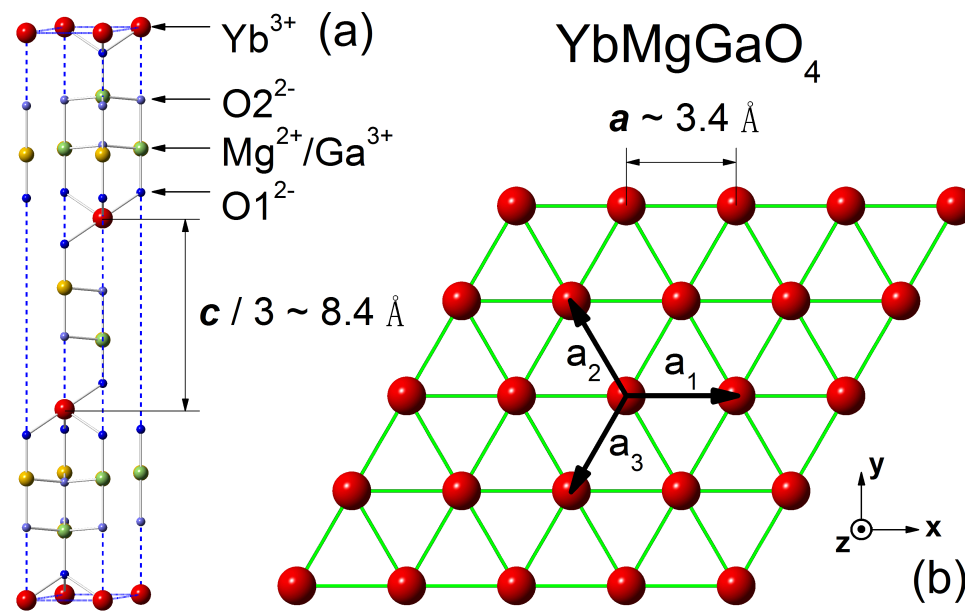
Chang-Le Liu
(Fudan)



Yaodong Li
(UCSB)

Changle Liu, Yao-Dong Li, GC, 1805.01865

Rare-earth triangular lattice magnets: spin liquid



with Yuesheng Li, Qingming Zhao,
Jun Zhao, Yao Shen, Yaodong Li

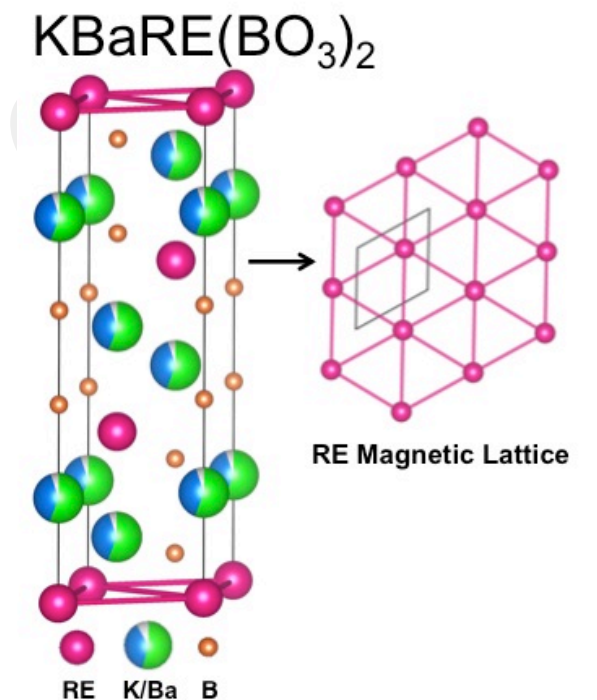
Rare-earth triangular lattice magnets: abundance

Compound	Magnetic ion	Space group	Local moment	Θ_{CW} (K)	Magnetic transition	Frustration para. f	Refs.
YbMgGaO ₄	Yb ³⁺ ($4f^{13}$)	$R\bar{3}m$	Kramers doublet	−4	PM down to 60 mK	$f > 66$	[4]
CeCd ₃ P ₃	Ce ³⁺ ($4f^1$)	$P6_3/mmc$	Kramers doublet	−60	PM down to 0.48 K	$f > 200$	[5]
CeZn ₃ P ₃	Ce ³⁺ ($4f^1$)	$P6_3/mmc$	Kramers doublet	−6.6	AFM order at 0.8 K	$f = 8.2$	[7]
CeZn ₃ As ₃	Ce ³⁺ ($4f^1$)	$P6_3/mmc$	Kramers doublet	−62	Unknown	Unknown	[8]
PrZn ₃ As ₃	Pr ³⁺ ($4f^2$)	$P6_3/mmc$	Non-Kramers doublet	−18	Unknown	Unknown	[8]
NdZn ₃ As ₃	Nd ³⁺ ($4f^3$)	$P6_3/mmc$	Kramers doublet	−11	Unknown	Unknown	[8]

YD Li, XQ Wang, GC*, PRB 94, 035107 (2016)

Magnetism in the KBaRE(BO₃)₂ (RE=Sm, Eu, Gd, Tb, Dy, Ho, Er, Tm, Yb, Lu) series: materials with a triangular rare earth lattice

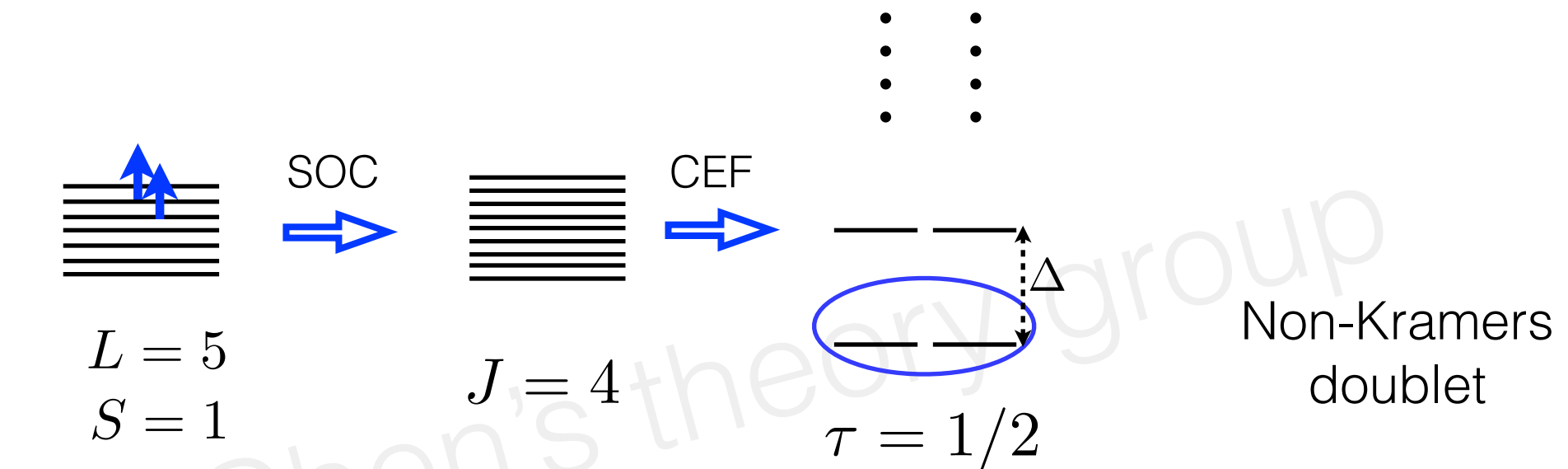
M. B. Sanders, F. A. Cevallos, R. J. Cava
Department of Chemistry, Princeton University, Princeton, New Jersey 08544



Ternary chalcogenides LiRS₂, NaRSe₂, KRSe₂, RbRSe₂,

.....

Non-Kramers doublets



$\text{Pr}^{3+}: 4f^2$

$$\begin{aligned} \mathcal{T} : S^z &\rightarrow -S^z \\ \mathcal{T} : S^{x,y} &\rightarrow S^{x,y} \end{aligned}$$

1. z component is the **dipolar** component, x,y are **quadrupolar** components
2. Only z (or Ising) component couples to external magnetic field.

Complete models for rare-earth triangular magnets

Usual Kramers doublet such as Yb ion in YbMgGaO₄

$$H = \sum_{\langle ij \rangle} J_{zz} S_i^z S_j^z + J_{\pm} (S_i^+ S_j^- + S_i^- S_j^+) + J_{\pm\pm} (\gamma_{ij} S_i^+ S_j^+ + \gamma_{ij}^* S_i^- S_j^-) \\ - \frac{iJ_{z\pm}}{2} [(\gamma_{ij}^* S_i^+ - \gamma_{ij} S_i^-) S_j^z + S_i^z (\gamma_{ij}^* S_j^+ - \gamma_{ij} S_j^-)]$$

Dipole-octupole doublet (not yet discovered, but should exist on triangular lattice)

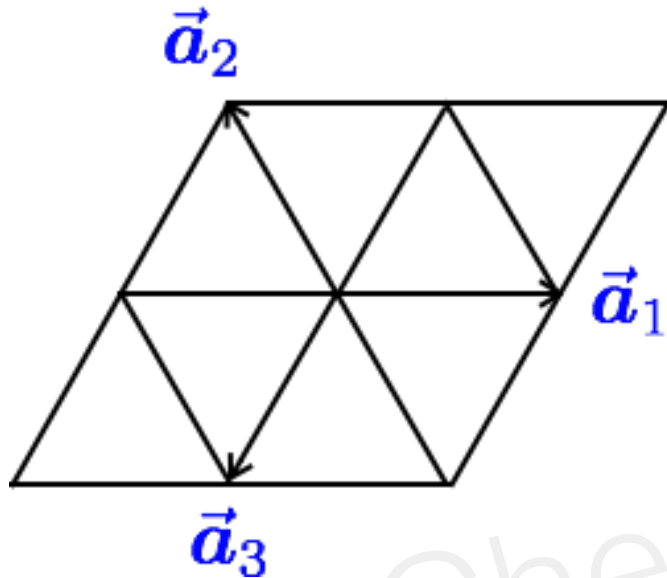
$$H = \sum_{\langle ij \rangle} J_z S_i^z S_j^z + J_x S_i^x S_j^x + J_y S_i^y S_j^y + J_{yz} (S_i^z S_j^y + S_i^y S_j^z)$$

Non-Kramers doublet

$$H = \sum_{\langle ij \rangle} J_{zz} S_i^z S_j^z + J_{\pm} (S_i^+ S_j^- + S_i^- S_j^+) \\ + J_{\pm\pm} (\gamma_{ij} S_i^+ S_j^+ + \gamma_{ij}^* S_i^- S_j^-),$$

Refs: Yao-dong Li, GC, etc, 2016-2017

Anisotropic spin model for non-Kramers doublet

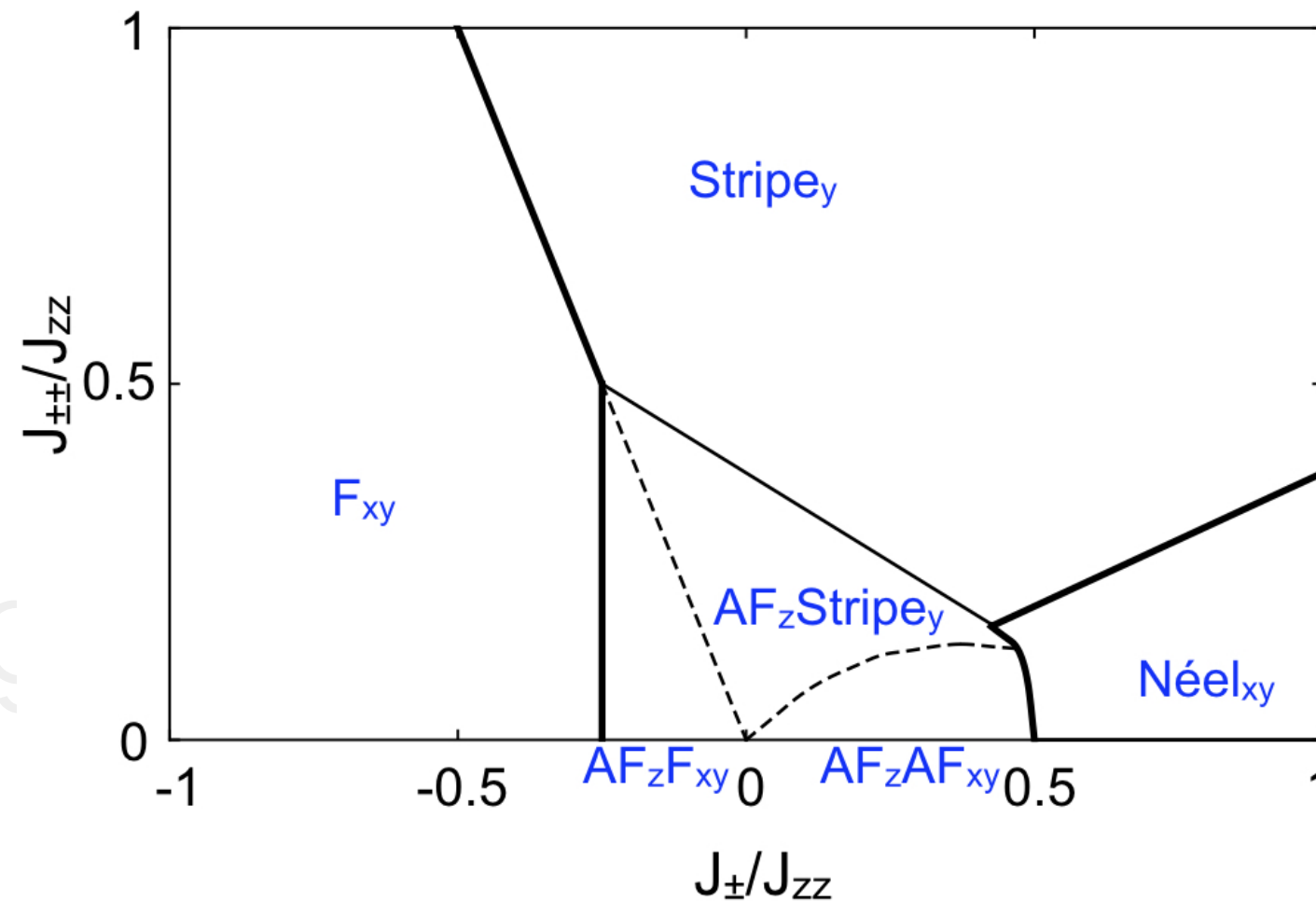


$$H = \sum_{\langle ij \rangle} J_{zz} S_i^z S_j^z + J_{\pm} (S_i^+ S_j^- + S_i^- S_j^+) \\ + J_{\pm\pm} (\gamma_{ij} S_i^+ S_j^+ + \gamma_{ij}^* S_i^- S_j^-),$$

in which, γ_{ij} is a bond-dependent phase factor, and takes 1, $e^{i2\pi/3}$ and $e^{-i2\pi/3}$ on the \mathbf{a}_1 , \mathbf{a}_2 and \mathbf{a}_3 bond (see

- * This model differs from the XXZ spin model by having an extra anisotropic spin interaction.
- * The model is anisotropic both in the spin space and in the position space. This is the consequence of the spin-orbit entanglement.
- * The spin components have distinct physical meanings.

Mean-field phase diagram



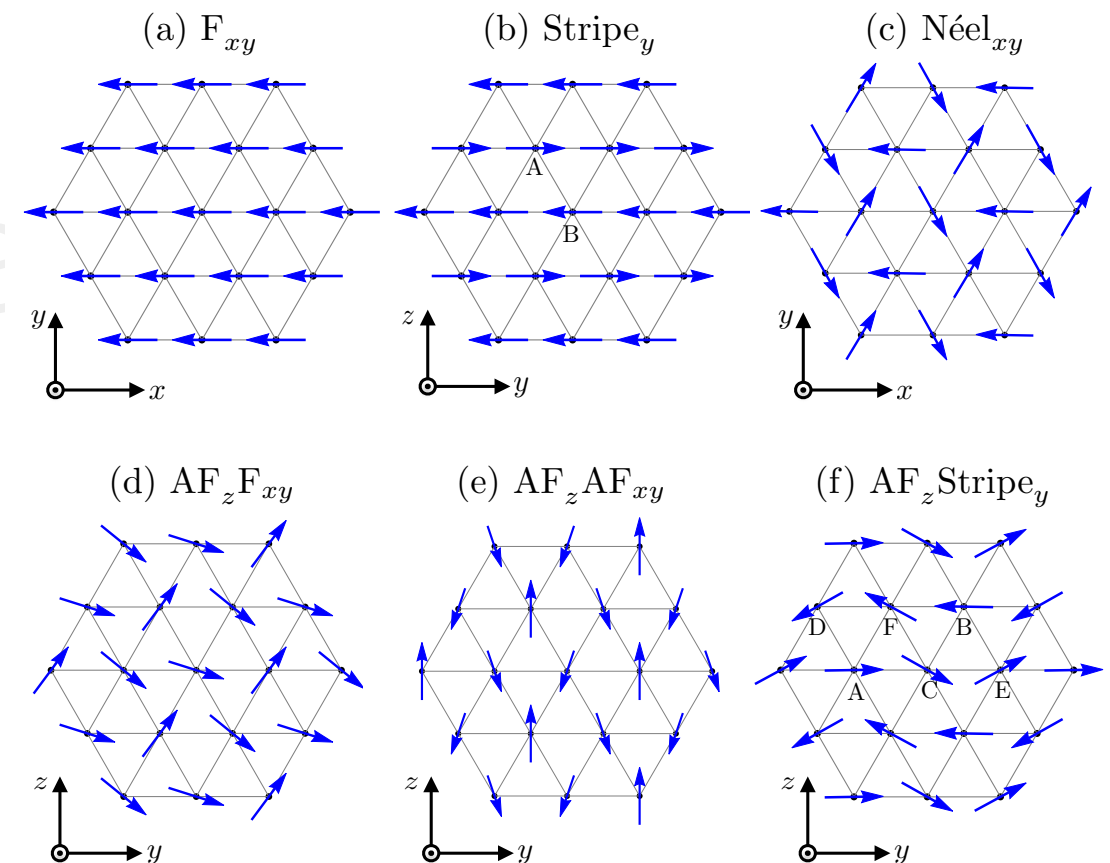
x,y components are quadrupole moments,
z component is dipole moment.

so, $AF_z AF_{xy}$ is antiferro-dipolar and antiferro-quadrupolar orders,
also known as super-solid in the XXZ limit.

List of magnetic phases

states	order types	elastic neutron
F_{xy}	pure quadrupolar	no Bragg peak
120° Néel	pure quadrupolar	no Bragg peak
Stripe_y	pure quadrupolar	no Bragg peak
$AF_z F_{xy}$	intertwined multipolar	Bragg peak at K
$AF_z AF_{xy}$	intertwined multipolar	Bragg peak at K
$AF_z \text{Stripe}_y$	intertwined multipolar	Bragg peak at K

TABLE II. The list of ordered phases in the phase diagram of Fig. 3.



Geometric frustration and multipolariness

The intertwined multipolar orders arises from the combination of geometrical frustration and the multipolar nature of the local moments.

With only geometrical frustration, the system would produce usual **dipolar** magnetic order.

With only spin-orbit-entangled local moments, the system would not have **intertwined** multipolar ordering structure.

What does neutron scattering measure?

The quadrupolar order is not directly visible from conventional magnetic measurement.

Despite this fact, the dynamical measurement is able to reveal the consequence of the quadrupolar orders.

What is essential here is the non-commutative relation between the dipole component and the quadrupole component.

The S_z component couples linearly with the external magnetic field. Likewise, the neutron spin would only couple to the dipole moment S_z . Therefore, the inelastic neutron scattering would measure the S_z - S_z correlation

$$\begin{aligned} \mathcal{S}^{zz}(\mathbf{q}, \omega > 0) \\ = \frac{1}{2\pi N} \sum_{ij} \int_{-\infty}^{+\infty} dt e^{i\mathbf{q} \cdot (\mathbf{r}_i - \mathbf{r}_j) - i\omega t} \langle S_i^z(0) S_j^z(t) \rangle \end{aligned}$$

Magnetic excitations

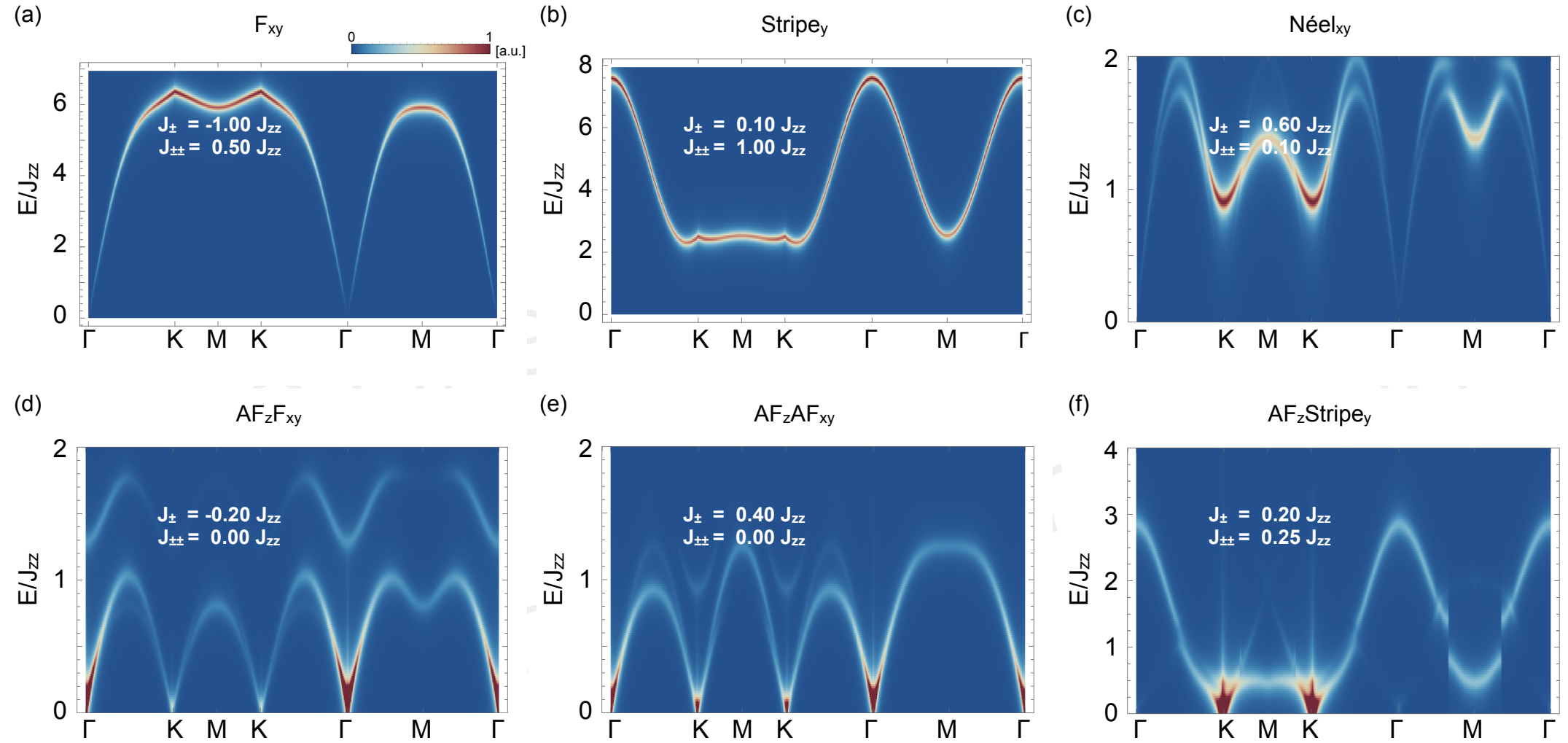
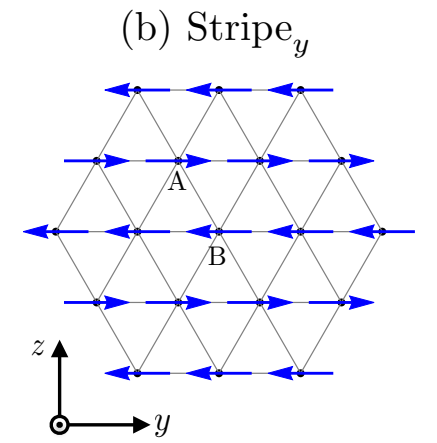


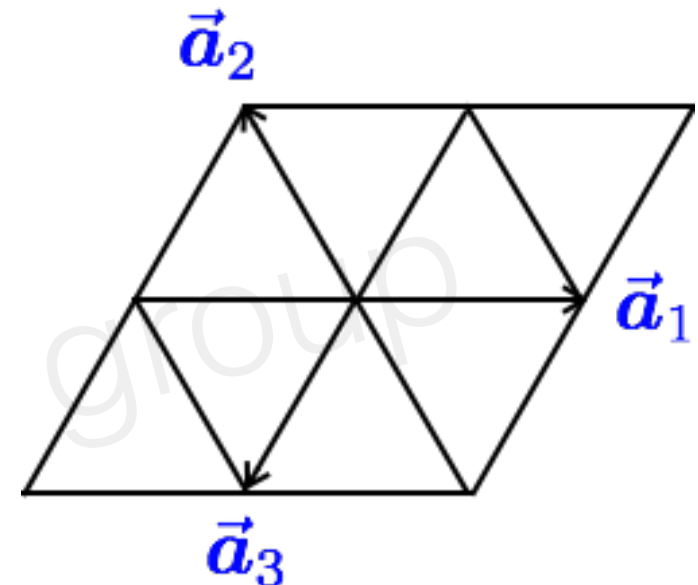
FIG. 6. Dynamic spin structure factors for the phases discussed in Sec. III, obtained from the linear spin wave theory. The representative parameters for different subfigures are given. The plots here are intensity plots. We also plot the full spin wave dispersions in Appendix. C.

Connection to Kitaev interactions

$$S_i^a \equiv \sqrt{\frac{2}{3}} S_i^x + \sqrt{\frac{1}{3}} S_i^z,$$

$$S_i^b \equiv \sqrt{\frac{2}{3}} \left(-\frac{1}{2} S_i^x + \frac{\sqrt{3}}{2} S_i^y \right) + \sqrt{\frac{1}{3}} S_i^z,$$

$$S_i^c \equiv \sqrt{\frac{2}{3}} \left(-\frac{1}{2} S_i^x - \frac{\sqrt{3}}{2} S_i^y \right) + \sqrt{\frac{1}{3}} S_i^z,$$



$$H = \sum_{\langle ij \rangle \in \alpha} \left[J \mathbf{S}_i \cdot \mathbf{S}_j + K S_i^\alpha S_j^\alpha \right. \\ \left. + \sum_{\beta, \gamma \neq \alpha} \Gamma (S_i^\alpha S_j^\beta + S_i^\beta S_j^\alpha + S_i^\alpha S_j^\gamma + S_i^\gamma S_j^\alpha) \right. \\ \left. + \sum_{\beta, \gamma \neq \alpha} (K + \Gamma) (S_i^\beta S_j^\gamma + S_i^\gamma S_j^\beta) \right],$$

So there are a lot of Kitaev materials !

Summary 2

1. In geometric frustrated system, intertwined multipolar orders could emerge.
2. The manifestation of the multipolar orders is rather non-trivial, both in the static and dynamic measurements.
3. The non-commutative observables/operators can be used to reveal the dynamics of hidden orders.